Theor. Appl. Climatol. 82, 153–176 (2005)
DOI 10.1007/s00704-005-0129-0

Theoretical and Applied Climatology
Printed in Austria

[1] Department of Oceanography, University of Cape Town, Rondebosch, South Africa
[2] Tanzania Meteorological Agency, Dar es Salaam, Tanzania

Relationships between intraseasonal rainfall variability of coastal Tanzania and ENSO

A. L. Kijazi[1,2] and **C. J. C. Reason**[1]

With 7 Figures

Received February 20, 2004; revised December 15, 2004; accepted December 16, 2004
Published online March 31, 2005

Summary

The influence of ENSO on intraseasonal variability over the Tanzanian coast during the short (OND) and long (MAM) rainy seasons is examined. In particular, variability in the rainfall onset, peak and end dates as well as dry spells are considered. In general, El Niño appears to be associated with above average rainfall while La Niña is associated with below average rainfall over the northern Tanzanian coast during OND, and to lesser extent MAM. Over the southern coast, the ENSO impacts are less coherent and this region appears to be a transition zone between the opposite signed impacts over equatorial East and southern Africa. The increased north coast rainfall during El Niño years is generally due to a longer than normal rainfall season associated with early onset while reduced rainfall during La Niña years tends to be associated with a late onset, and thus a shorter than average rainfall season. Wet conditions during El Niño years were associated with enhanced convection and low-level easterly anomalies over the equatorial western Indian Ocean implying enhanced advection of moisture from the Indian Ocean while the reverse is true for La Niña years. Hovmöller plots for OLR and zonal wind at 850 hPa and 200 hPa show eastward, westward propagating and stationary features over the Indian Ocean. It was observed that the propagating features were absent during strong El Niño years. Based on the Hovmöller results, it is observed that the convective oscillations over the Tanzanian coast have some of the characteristic features of intraseasonal oscillations occurring elsewhere in the tropics.

1. Introduction

The economy of Tanzania depends significantly on rain fed agriculture, which is highly vulnerable to the amount and distribution of rainfall. Both spatial rainfall anomalies over the region and temporal variability within the wet season itself can be prominent and lead to significant deficiencies. In some areas of Tanzania, agriculture is limited by the length of the rain season while in others it is amount limited (Mhita, 1984). Intraseasonal rainfall forecasts can assist farmers in decisions regarding planting, fertilising, pesticide application, and irrigation demand. Preliminary work on the onset and end of the rainfall seasons over Tanzania has been done by Alusa and Gwange (1978) and Mhita and Nassib (1987) but there is a need for investigation into the possible impacts on intraseasonal rainfall of the El Niño Southern Oscillation (ENSO) and other large scale modes.

On interannual scales, it has long been established that ENSO modulates rainfall variability over East Africa (e.g. Ropelewski and Halpert, 1987; Janowiak, 1988; Ogallo, 1988; Hastenrath et al., 1993; Hutchinson, 1992; Nicholson and Kim, 1997; Indeje et al., 2000; Mutai and Ward, 2000; Amissah-Arthur et al., 2002). Recently, Hastenrath and Polzin (2004) have shown that East African rainfall during the OND season is related to the strength of the equatorial surface westerlies over the Indian Ocean and the zonal pressure gradient across the basin. Both of these variables are modulated during ENSO as well as during other modes such as the Indian Ocean Zonal Mode (Webster et al., 1999) or tropical dipole mode (Saji et al., 1999), which also impacts strongly on East African OND rainfall. Typically, rainfall tends to be enhanced (reduced) over equatorial East Africa during El Niño (La Niña) events (e.g. Camberlin, 1995; Nicholson, 1996). Given the strong evidence of significant ENSO signals in the Indian Ocean (e.g. Cadet, 1985; Nicholson and Kim, 1997; Tourre and White, 1997; Reason et al., 2000) and over much of East Africa, an ENSO influence on East African intraseasonal rainfall variability might also be anticipated.

Intraseasonal oscillations (ISO) in the atmosphere are generally defined as fluctuations with periods longer than the synoptic scale but shorter than the seasonal time scale and are a prominent feature of tropical weather particularly in the Indo-Pacific region (Madden and Julian, 1971, 1994; Vincent et al., 1991). Initially identified by Madden and Julian (1971) they have become widely studied in recent times. However, most previous work on East African climate associations with ENSO has looked at seasonal anomalies. With the exception of Mpeta and Jury (2001), relatively little research has been conducted on Tanzanian intraseasonal variability although some work has been done for other countries in southern Africa (e.g. Matarira and Jury, 1992 for Zimbabwe; Levey and Jury, 1996 for South Africa). Previous work did not look at how ENSO influences the intraseasonal variability of Tanzania and therefore this study intends to address that gap by attempting to investigate the ISO responsible for short-term rainfall variability in the Tanzanian coast during ENSO years. In particular, there is interest in the relationships between the ISO and ENSO, e.g. are El Niño and La Niña years characterised by coherent differences in intraseasonal wet and dry spells over Tanzania?

Studies of ISO which link tropical Africa and the adjacent oceans include Zhu and Wang (1993) who observed two prominent action centres in the central Indian and western Pacific oceans for tropical 30–60 day convective variability. Anyamba (1992) identified a 20–30 day oscillation in the tropical outgoing long wave radiation (OLR) spectra in the western Indian Ocean and found that while the 40–50 day ISO is characterized by an eastward propagating wave in the Indian and West Pacific Oceans, the 20–30 day ISO has a much weaker zonal propagation. Rui and Wang (1990) documented the development and dynamic structure of typical intraseasonal convection anomalies using pentad OLR and ECMWF derived 200 and 850 hPa wind divergence. Mpeta and Jury (2001) found that convective events over southwestern Tanzania were associated with an influx of northeasterly Indian Ocean monsoon flow followed by increased westerly flow from the Guinea/Congo region.

The area of Tanzania studied herein is bounded by latitudes 4–12° S and longitudes 38.5–41° E. Two main rainy seasons are experienced in the north coast (4–8° S), the long rains (March–May) and the short rains (October–December), and these are associated with the northward and southward movement of the ITCZ respectively. The south coast (8–12° S) experiences one rain season from November to April and appears to be a transition region in its ENSO response between the opposite signed rainfall impacts of equatorial East Africa and tropical–subtropical southeastern Africa.

2. Data and methods

NCEP gridded data for 1970–1999 were used to provide insight into the circulations associated with onset, peak and withdrawal of rainfall. NOAA OLR data, together with rainfall station and CMAP data, were used to explore the influence of ENSO on Tanzanian coastal rainfall. CMAP data, which are available from 1979 onwards, are a merge of satellite, model and rain gauge data at 2.5° resolution (Xie and Arkin, 1997) whereas the rainfall station data used consists of monthly totals obtained from the Tanzania Meteorological Agency. The latter includes observations from 10 rainfall stations scattered throughout the coastal region of Tanzania. The period 1970–1999 was selected for analysis since all stations had continuous quality records.

In order to investigate the influence of ENSO on Tanzanian coastal rainfall, the normalised and spatially averaged rainfall indices for the north and south coasts (Fig. 1) were developed using the means and standard deviations of the station data. A departure of at least 1 standard deviation above (below) the mean defines an anomalously wet (dry) season. Consistency of these results were checked with CMAP data for the overlapping 1979–1999 period.

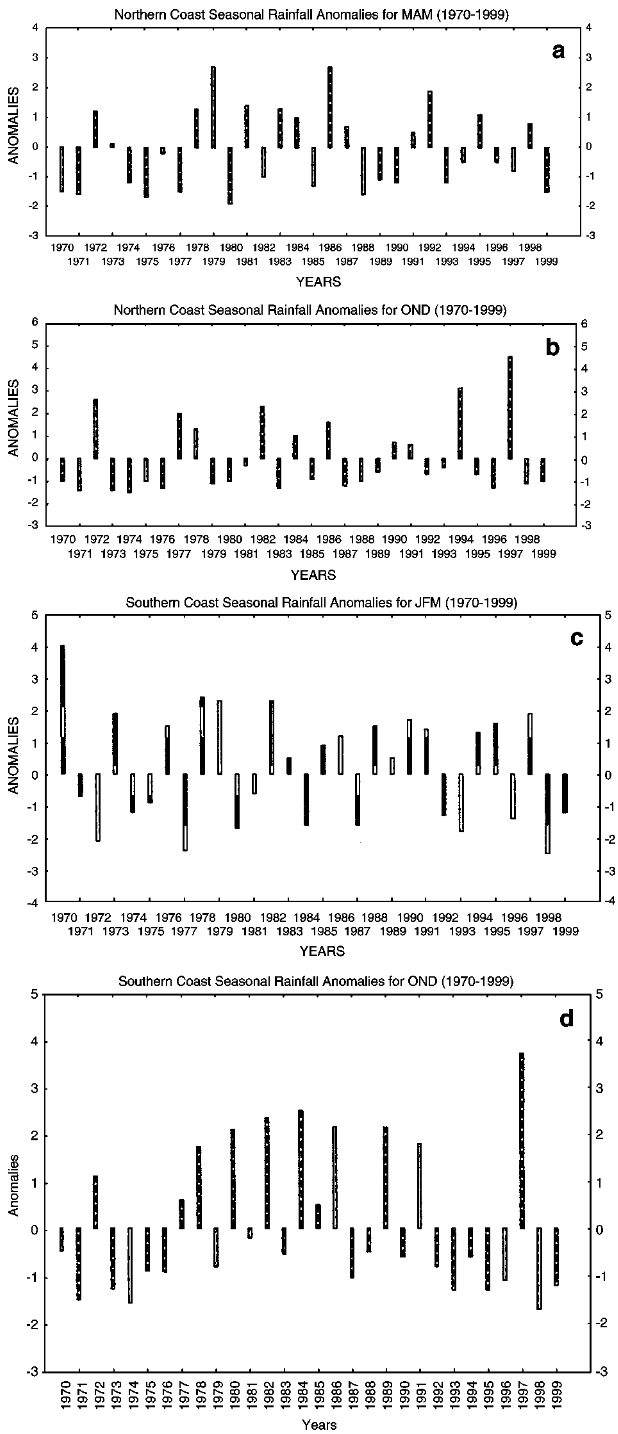

Fig. 1. Time series of normalised station rainfall anomalies for **a**) north part (4–8° S) of coast MAM season, **b**) north coast OND season, **c**) south part (8–12° S) of coast JFM season, **d**) south coast OND season

Moisture fluxes were derived from the product of specific humidity and the horizontal wind vector using NCEP re-analyses. However, due to the fact that NCEP has probable errors in specific humidity and there are relatively few tropical African observations for assimilation into the model (Kalnay et al., 1996), this study will focus more on the sign than on the magnitude of the moisture flux.

To remove diurnal variability, the analyses use 5 day pentads beginning with pentad 1 (1–5 January) of a given year and ending at pentad 73 (27–31 December). Pentad 12 contains an additional day to include February 29 in the case of a leap year. CMAP data is used for the pentad analysis since the station data are only available as monthly totals. Mean values and anomalies of pentad rainfall were calculated separately for the north and south coasts. Pentad area-averaged rainfall time series were inspected and rainfall onset peak and end dates derived as per Table 1.

Table 1. Criteria used to define onset, peak and end dates of the rainy season

North coast short rain season (OND)

Onset: 5-day rainfall at least 7.5 mm followed by three consecutive pentads having rainfall amount of not less than 5 mm/pentad.

Peak: The pentad with highest amount of rainfall in the season.

End: If three consecutive pentads have mean rainfall of 2 mm/day or less, the preceding pentad is considered to be the end of rain season.

Dry spell: 5-day rainfall less than 7.5 mm.

North coast long rain season (MAM) and south coast November to May season

Onset: 5-day rainfall exceeds 10 mm followed by three consecutive pentads having rainfall amount of not less than 10 mm/pentad.

Peak: The pentad with highest amount of rainfall in the season.

End: If three consecutive pentads have mean rainfall $\leq$2 mm/day the preceding pentad is considered to be the end of rain season.

Dry spell: 5-day rainfall less than 10 mm.

Note: The pentad preceding the onset pentad is considered as the pre-onset

These criteria have been found by the Tanzanian Meteorological Agency to be appropriate for the region. These dates were used for analyses of the regional circulation associated with the pentads corresponding to pre-onset (one pentad prior to onset, $P-1$), onset (P0), peak (P1) and end $(P+1)$ of the rainfall season.

Longitude-time diagrams or Hovmöller plots of OLR and zonal wind at 850 and 200 hPa are used to identifying zonally propagating ISO. These plots were constructed for various ENSO years for both the short rain (OND) and the long rain season (MAM) starting from one month before the season and ending one month after the season. To isolate the ISO, the data used in these Hovmöller analyses were first subjected to a 30–50 day band pass filter using the Dolph – Chebyshev convergence window (Doblas-Reyes and Déqué, 1998).

3. Seasonal anomalies

In general, Fig. 1a–b indicates that El Niño years are associated with above normal rainfall and La Niña years are associated with below normal rainfall for the north coast. The OND signals appear to be more robust and coherent than those during the MAM wet season. The years 1972, 1982, 1986, 1994 and 1997 are identified as El Niño years with more than one standard deviation departure from the mean for the north coast while 1970, 1973, 1975, 1988 and 1998 are the corresponding La Niña years. OND 1997 stands out as the wettest season and coincides also with a positive Indian Ocean Zonal Mode event. For the MAM season, most mature phase El Niño (La Niña) years correspond to above (below) average north coast rainfall.

For the south coast, the OND season seems to show similar ENSO impacts to the north coast, except for 1990 and 1994, and inspection also suggests a quasi-decadal signal in the anomalies (Fig. 1d). A less coherent signal is evident for the JFM season for the south coast (Fig. 1c) with 1973, 1983 and 1995 representing mature phase El Niño years with above average rainfall and 1987, 1992 and 1998 years with below average conditions. A similar mixed response is evident for the mature phase La Niña years. This mixed response may arise as the south coast appears to be a transition region between the different ENSO signals in equatorial East and tropical–subtropical southeastern Africa. Given the mixed signals over the south coast, focus here is placed on analysis of the ISO for the north coast.

4. Hovmöller analyses

Longitude time plots of 30–50 day filtered OLR, lower and upper level zonal wind anomalies were derived for the El Niño years of 1982, 1986, 1994 and 1997 (1972 is not included since OLR data are not available) and reveal alternating positive and negative features for each year. Figure 2a shows examples for the 1982/83 and the 1986/87 seasons (the others are not shown for brevity). This period of filtering was found to be optimal (20–40, 20–60 and 40–60 days were also tried) and roughly spans the 40–50 and near 30 day peaks in tropical convection and upper air parameters derived by Hayashi and Golder (1993). Figure 2a often indicates eastwards propagating anomalies between September and December over the central Indian Ocean (70°–100° E) while westward propagating anomalies were sometimes observed between the Tanzanian coast and 70° E. These propagating features may be convectively coupled equatorial Kelvin, $n=1$ equatorial Rossby or mixed Rossby-gravity waves (Madden and Julian, 1994; Wheeler and Kiladis, 1999; Wheeler and Weickmann, 2001). Stationary features dominated 1997, which was the wettest year during the period of study and also occurred in 1982, particularly in the central Indian Ocean. This result suggests that propagating features occur less often during particularly strong El Niños and wet OND seasons in Tanzania.

It is seen that the largest OLR negative anomaly values (below $-20\,\mathrm{W/m^2}$) occur between 70 and 120° E, indicating that more active convection occurs towards the maritime continent over the central and eastern tropical Indian Ocean as found by other researchers (e.g. Rui and Wang, 1990). Westward propagating negative OLR anomalies over the western Indian Ocean propagate with a mean speed of about $2\,\mathrm{m/s}$ and are associated with strong convection over the Tanzanian coast and increased rainfall during El Niño years. Eastward propagating features were found to have different phase speeds in different years and over different areas. They generally propagate between $2–6\,\mathrm{m/s}$ with mean speed of about 3 m/s or slightly slower than typical eastward propagation in the Indian Ocean region (Madden and Julian, 1994).

Areas of large negative OLR anomalies (strong convection) couple well with areas of strong westerly anomalies at 850 hPa and strong easterly anomalies at 200 hPa. Such an association has been found in previous studies of tropical intraseasonal oscillations (e.g. Rui and Wang, 1990; Knutson and Weickmann, 1987). The combination of strong convection over the Indian Ocean with westerly wind anomalies at lower levels coupled with easterly wind anomalies in the upper levels implies a well-established Indian Ocean Walker cell during the OND season, consistent with the findings of Hastenrath (2000).

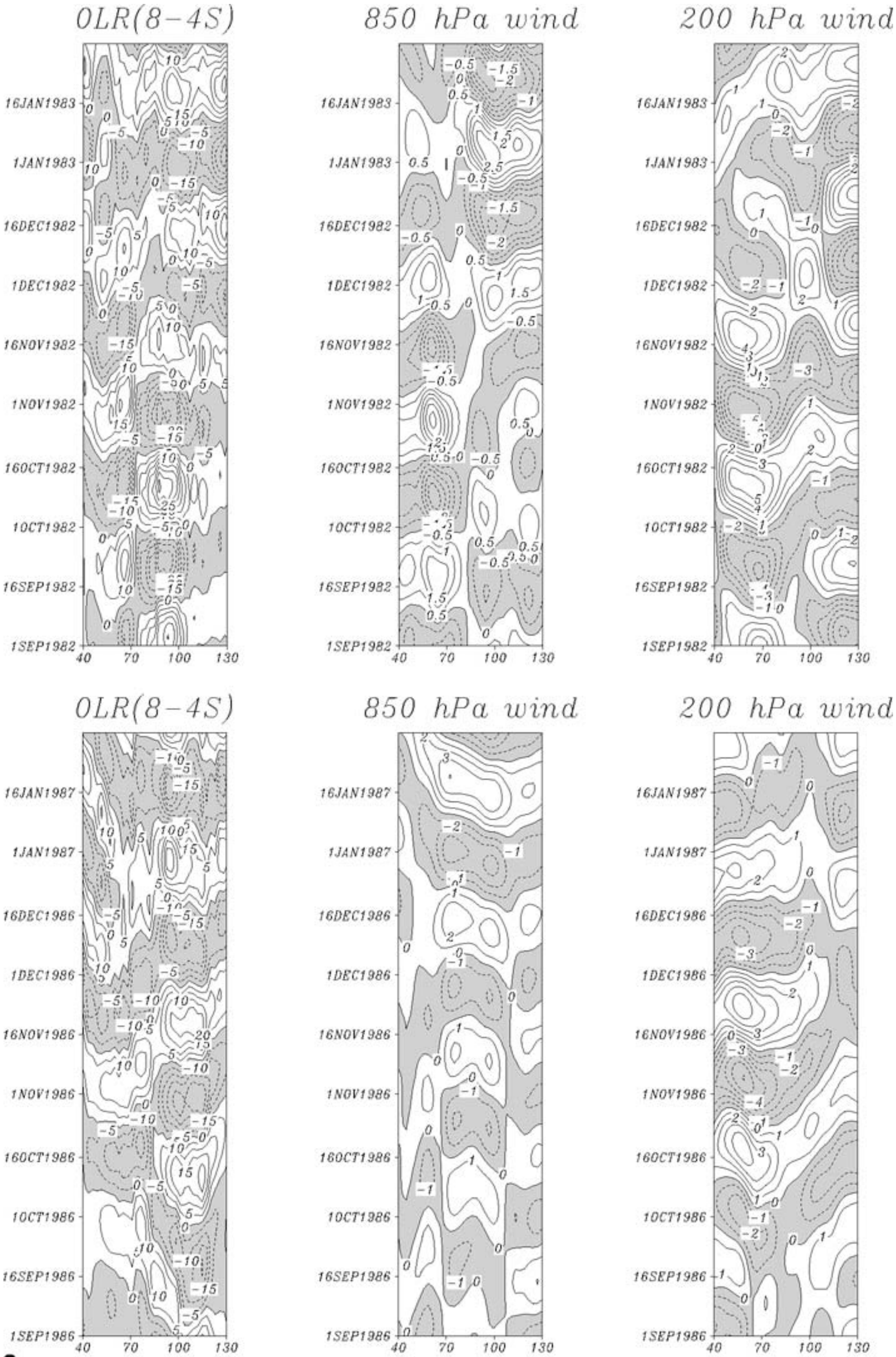

a

Fig. 2. Hovmöller plots of bandpass filtered OLR, zonal wind at 850 hPa and 200 hPa for 1982/83 and 1986/87 El Niño years during **a**) OND and **b**) MAM season. Contour intervals are 5 Wm^{-2}, 0.5 m/s and 1 m/s respectively. Shaded areas represent negative anomalies

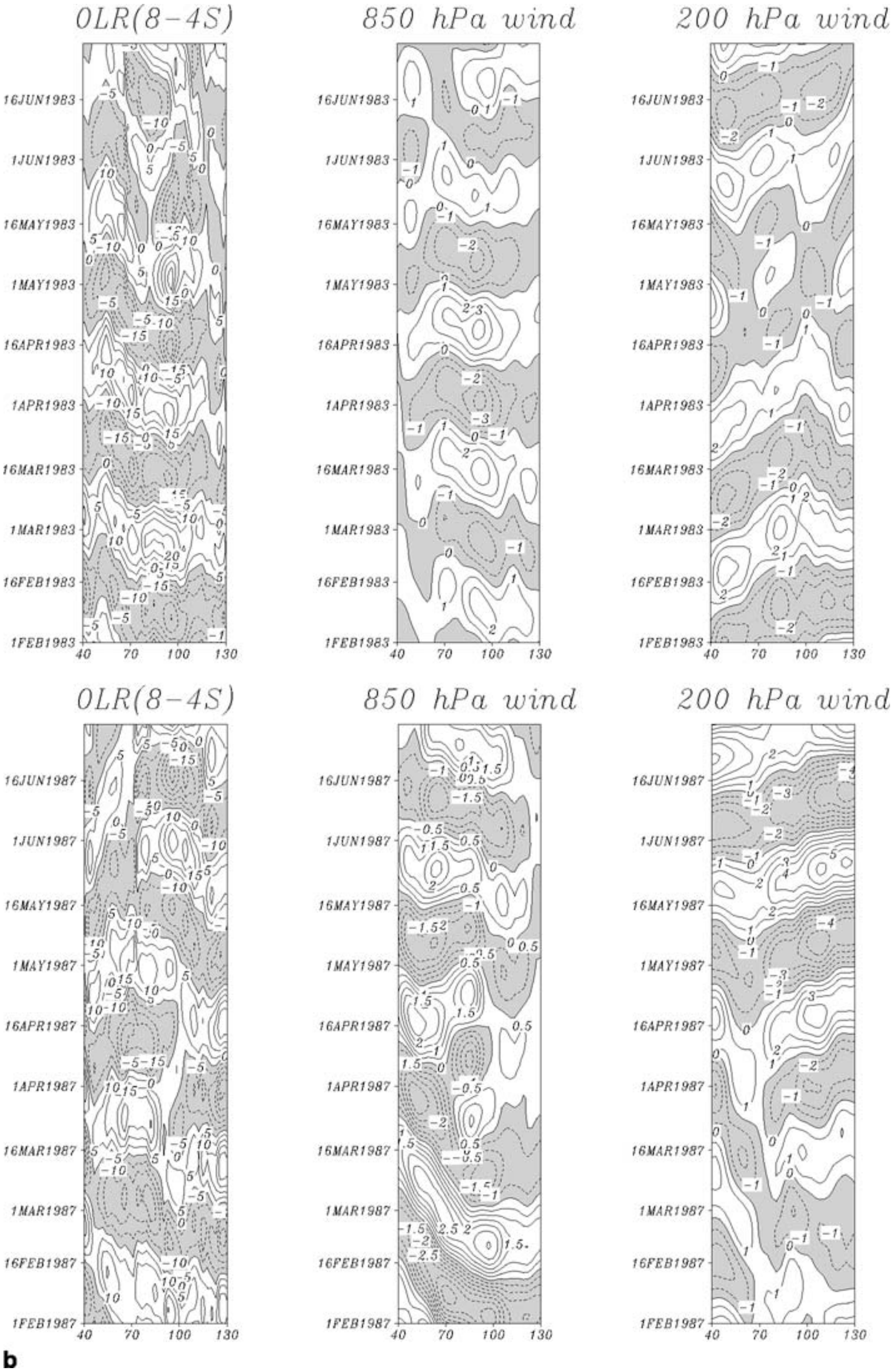

Fig. 2 (*continued*)

Longitude time plots of 30–50 days filtered OLR, 850 and 200 hPa zonal wind anomalies for mature phase El Niño years 1983, 1987, 1995 and 1998 are shown in Fig. 2b. Alternating positive and negative OLR anomalies are a common feature of most years except in 1983 between May and June when disorganised patterns were observed. Eastward propagating negative and positive OLR anomalies were observed in 1994 and 1997 with a mean phase speed of 2 m/s. Westward propagating features, which seem to originate from near 80° E, were mainly observed in 1983 and 1987.

Stationary features tend to dominate the 850 hPa wind over the central Indian Ocean between March and May with westward propagating features over the western Indian Ocean (less obvious in 1983). At 200 hPa, the dominant aspect was eastward propagating positive and negative wind anomalies except in 1987 where well-defined westward propagating features were observed between February and April. As for the OND season, the areas of large negative OLR anomalies (strong convection) couple well with areas of strong westerly anomalies in lower levels with strong easterly anomalies in upper levels, which leads to increased rainfall over the Tanzanian coast.

Filtered OLR and wind anomalies for La Niña and mature phase La Niña years were also constructed (not shown). As for the El Niño seasons, alternating positive and negative OLR anomalies were observed with both propagating and stationary features occurring. Eastward propagating features were observed to be the dominant pattern in both 850 and 200 hPa zonal winds except for 1999 when westward propagating anomalies were observed between March and June.

Two differences in the oscillations are apparent between El Niño and La Niña years. First, the eastward propagating OLR anomalies seem to have high phase speed during La Niña years, a good example is 1999 (7 m/s). Secondly, eastward propagating OLR anomalies dominated the western Indian Ocean during La Niña years, a good example is 1988/89 while for the El Niño years the anomalies maintain westward propagation (e.g. 1982/83, 1986/87). The presence of eastward propagating OLR anomalies over the western Indian Ocean during La Niña years leads to suppressed convection and drier conditions over the Tanzanian coast since it implies moisture convergence and unstable conditions significantly offshore rather than over the land.

5. Intraseasonal rainfall variability and criteria for rainfall onset, peak and end

The CMAP pentad rainfall data are averaged between 38.5°–41° E, 4°–8° S for the north coast and between 38.5° –41° E, 8°–11° S for the south coast. CMAP data are used for this purpose as only monthly data are available for the stations; however, this restricts the analysis to 1979 onwards. Figure 3a represents the climatological time series of pentad rainfall over the Tanzanian north coast while El Niño and La Niña OND composites and the following El Niño + 1 and La Niña + 1 MAM composites for the north coast are shown in Fig. 3b. Rainfall time series for each individual El Niño and La Niña year during OND and MAM seasons and preceding months were also derived and plotted but are not shown for brevity. The rainfall onset, peak and end (withdrawal) dates (Tables 2–4) were extracted from each of these time series using the criteria listed in Table 1.

Table 2 indicates that for the north coast OND season, the rainfall starts almost a month earlier than climatology during the El Niño years, these seasons reach their peak pentad about the same time as the mean, and this peak receives a large amount of rainfall (7 mm/day) (Fig. 3b). Only one significantly dry pentad occurs during El Niño OND seasons. By contrast, the La Niña years start the rainy season two pentads later than the mean, reach their peak pentad over a month later than average with reduced values (around 4 mm/day) and, as a result of a shorter season and reduced intensity, receive below average rainfall. In addition, the La Niña OND seasons are characterised by three dry spells as compared to only one on average for climatology or El Niño seasons. Note that there is no difference in the end date of the OND season for any of the three categories in Table 2; thus, the major ENSO influence seems to be on the onset date and the intensity of the OND rains.

During the north coast MAM season (Table 3), the onset for the El Niño + 1 composite was three pentads late but the amount received was higher than average with maxima of about 9 mm/day (Fig. 3b) as opposed to 5–6 mm/day in the climatological plot, and this peak was one pentad later than average. For the La Niña + 1 years, onset occurs at about the same time as the climatological mean but the amount received was more variable (maxima 7–8 mm/day) and the peak pentad is substantially later than average. Neither the El Niño + 1 nor the La Niña + 1 seasons experienced any significant dry pentads and both finished one pentad earlier than climatology.

Plots of individual ENSO OND and MAM seasons show that each event has its own characteristics in terms of onset, peak and end of the rainy season and dry spells as listed in Table 4. With the exception of 1986, all El Niño OND

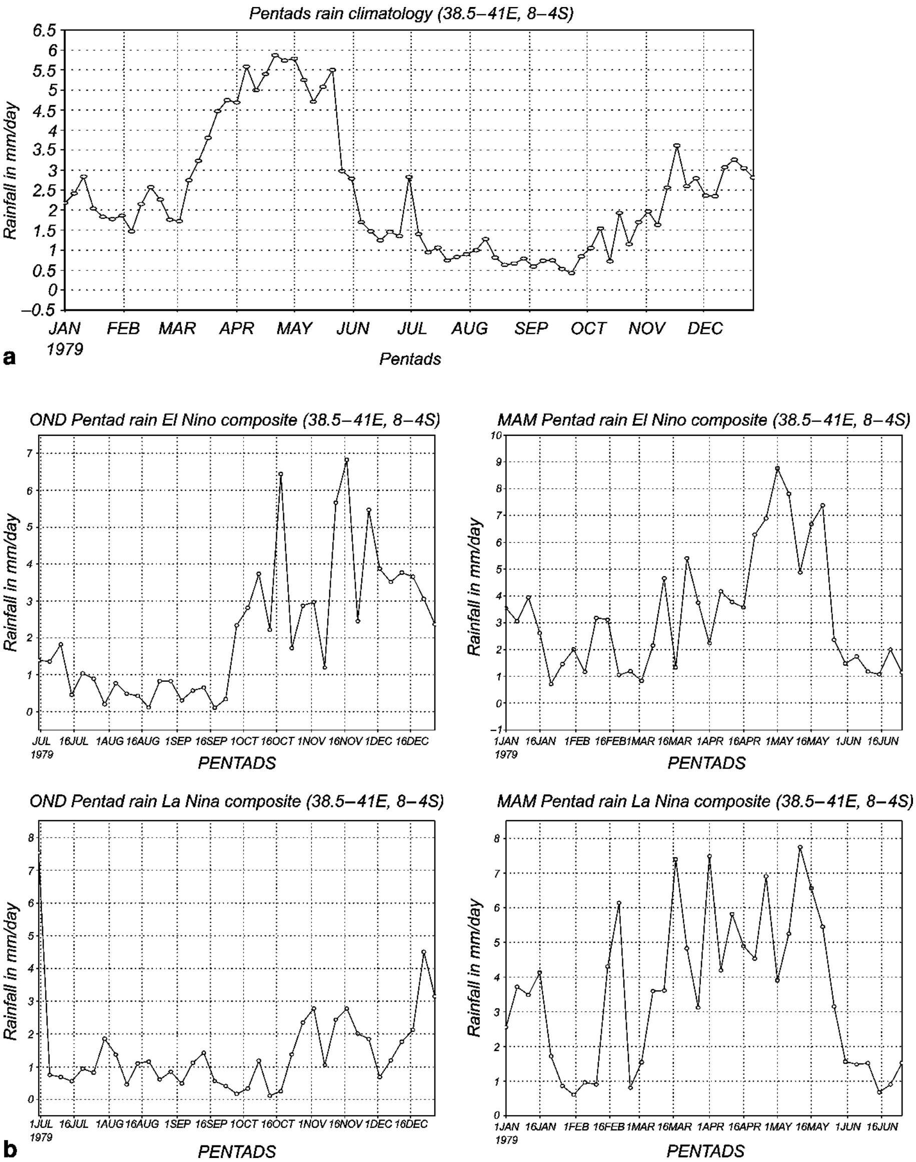

Fig. 3. a) Climatological pentad CMAP rainfall time series for north coast of Tanzania, **b**) north coast pentad rainfall time series for El Niño/La Niña and El Niño + 1/La Niña + 1 composites

Table 2. Rainfall onset, peak, end and major dry spell dates as derived from CMAP data for OND for the north coast

Events	Climatology	El Niño composite	La Niña composite
Pre-onset	58^{th} Pentad	54^{th} Pentad	60^{th} Pentad
(P − 1)	(13–17 October)	(23–27 September)	(23–27 October)
Onset	59^{th} Pentad	55^{th} Pentad	61^{st} Pentad
(P0)	(18–22 October)	(28 Sept.–02 October)	(28 October–01 Nov.)
Peak	65^{th} Pentad	65^{th} Pentad	72^{nd} Pentad
(P1)	(17–21 November)	(17–21 November)	(22–26 December)
End	4^{th} Pentad	4^{th} Pentad	4^{th} Pentad
(P + 1)	(16–20 January)	(16–20 January)	(16–20 January)
Major dry	60^{th} Pentad	63^{rd} Pentad	63^{rd}, 68^{th}–69^{th} Pentad
Pentads	(23–27 October)	(07–11 November)	(07–11 Nov., 02–11 Dec.)

seasons are found to have an early onset. This does not always translate into a longer rainy season since some OND seasons end earlier than average, and in fact, 1994 had a season that lasted one pentad shorter than climatology and 1986 was the same duration. However, in 1997,

Table 3. As for Table 2 but MAM season for the north coast (MAM season)

Events	Climatology	El Niño composite	La Niña composite
Pre-onset (P − 1)	13th Pentad (02–06 March)	16th Pentad (17–21 March)	13th Pentad (02–06 March)
Onset (P0)	14th Pentad (07–11 March)	17th Pentad (22–26 March)	14th Pentad (07–11 March)
Peak (P1)	24th Pentad (26–30 April)	25th Pentad (01–05 May)	27th Pentad (11–15 May)
End (P + 1)	31st Pentad (31 May–4 June)	30th Pentad (26–30 May)	30th Pentad (26–30 May)
Major dry Pentads	0	0	0

Table 4. As for Table 2 but for each ENSO (north coast OND season) and ENSO + 1 (north coast MAM season) year. E and L represent El Niño and La Niña year respectively with corresponding following year E + 1 and L + 1

Year	Pre-onset pentad (P − 1)	Onset pentad (P0)	Peak pentad (P1)	End pentad (P + 1)	Major dry pentads
1982 (E)	54th	55th	57th	3rd (1983)	61st–63rd, 70th, 2nd (1983)
1986 (E)	58th	59th	67th, 69th and 71st	4th (1987)	61st, 63rd, 68th, and 73rd
1994 (E)	57th	58th	69th	2nd (1995)	65th and 66th
1997 (E)	54th	55th	59th	10th (1998)	60th, 63rd, and
	23–27 Sept	28 Sep–02 Oct	18–22 Oct	15–19 Feb	5th (1998)
1983 (E + 1)	16th	17th	24th	33rd	22nd and 26th
1987 (E + 1)	19th	20th	26th	32nd	30th and 31st
1995 (E + 1)	19th	20th	30th	30th	26th
1998 (E + 1)	16th	17th	23rd	26th	0
	17–21 March	22–26 March	21–25 April	06–10 May	
1988 (L)	61st	62nd	73rd, 5th (1989)	5th (1989)	66th and 67th
1995 (L)	59th	60th	61st	2nd (1996)	63rd, 64th, 68–70th and 73rd
1998 (L)	SEE NOTE BELOW				
1999 (L)	62nd	63rd	64th	71st	68th and 69th
1989 (L + 1)	18th	19th	22nd	30th	0
1996 (L + 1)	13th	14th	28th	29th	26th
1999 (L)	12th	13th	24th	31st	28th
2000 (L)	15th	16th	24th	27th	22nd

Note: In 1998, the onset and end of rainfall were undefined as the whole season was dry except 65th, 66th and 67th pentads, which recorded rainfall

which was the wettest year during the period of study, the rainfall started about three weeks before and the withdrawal was one month later than climatology. This season stands out as unusually long (by comparison, 1982 was three pentads longer than average). Of these four seasons, all except 1986 were also an Indian Ocean Zonal Mode year so it does not appear to be the combination of this mode with a strong El Niño that is responsible for 1997 being so unusual in this respect. OND 1997 and 1986 were also unusual in that wet spells were more closely spaced (1–2 pentads apart) than for 1982 and 1994 which showed generally longer spacing, with one dry spell of seven and five pentads respectively. In terms of OND totals after onset, 1982 (310 mm) represents the wettest OND El Niño season after 1997 (480 mm), and 1994 (210 mm) was the least wet.

Turning to the La Niña OND seasons, these have a shorter rainfall season than average which results from a late onset and a generally early withdrawal (except 1988 which ended one pentad later). Major wet spells also seem to be more widely spaced in time than for the El Niño OND seasons. An extreme example is 1998, when the length of the rainfall season was only about two weeks. None of the four La Niña seasons correspond to a negative Indian Ocean Zonal Mode year. In order of increasing dryness after onset, the seasons are 1988 (155 mm), 1995 (140 mm), 1999 (105 mm) and 1998 (90 mm for the whole season – the onset criterion was never satisfied in this case). In general, the common feature for all La Niña years is below average rainfall during the season while El Niño years show above average rainfall during the north coast OND season.

For the MAM season, all El Niño years were delayed in starting the rains but two finished late and two early compared to climatology. The major wet spells are also more widely spaced than for the OND season and all MAM seasons experienced at least one dry pentad. After onset, the wettest seasons were 1983 and 1998 and the least wet 1995. By comparison, two of the La Niña seasons started late and one early, and all but 1999 ended rather earlier than average. Each season except 1989 had one dry pentad and the major wet spells for this season were more closely spaced in time than for the other three cases. After onset, the wettest season was 1999 and the driest 1989 and 2000. For the MAM season, ENSO rainfall impacts over the north coast appear more variable than those during OND.

The dates given in Table 4 are used to define the periods for which NCEP re-analyses are composited in order to try and understand the circulation patterns associated with the onset, peak and withdrawal stages of the rainy season.

5.1 ENSO influence on the short rains (OND)

Figure 4a–d show NCEP anomalies in OLR, 850 hPa moisture flux, middle and upper level wind for the El Niño years and Fig. 5a–d the corresponding La Niña seasons. To qualify for compositing, El Niño and La Niña years need to show a north coast station averaged rainfall anomaly of at least 1 standard deviation during the OND season (Fig. 1b). The resulting El Niño years for the OND composite are 1972, 1982, 1986, 1994 and 1997 with the corresponding La Niña years being 1970, 1973, 1975, 1988, 1998 and 1999. The pentads used are the same as those used above with the dates for the El Niño and La Niña composites shown in Tables 2–4.

One pentad before the onset of the OND rain season (P – 1) (Fig. 4a), much of the western Indian Ocean is covered by positive OLR anomalies with the highest anomaly value of the order of 40 W/m^2 observed over the equatorial central Indian Ocean. At 700 hPa, the easterly wind anomalies over this region oppose the mean flow, implying convergence and subsidence down through the lower atmosphere. Most of the western Indian Ocean is characterized by an anticyclonic moisture flux anomaly that results in northwesterly to northerly anomalies near the Tanzanian coast. As a result, there is little penetration of moisture inland, which is consistent with positive OLR anomalies over Kenya and northern Tanzania. At 200 hPa, easterly wind anomalies exist over much of Tanzania, thereby opposing the background flow and implying convergence, and hence subsidence down through the atmosphere, suppressing convection.

By the onset of the OND rain season (P0) (Fig. 4b), a deep convective zone has developed over the equatorial western Indian Ocean, as indicated by negative OLR anomalies over the region. Enhanced moisture flux convergence over the Tanzanian coast, as indicated by northeasterly anomalies over the Kenyan and north Tanzanian coasts, which also imply less export of moisture away from East Africa over the equatorial western Indian Ocean, results in increased rainfall over the north coast at the onset of the rainfall season. In addition to the convective zone near 55–65° E, a developing area of convection is now apparent over coastal East Africa. Over the equatorial Indian Ocean, easterly anomalies are evident at both 850 and 700 hPa consistent with a weaker zonal pressure gradient across the basin and enhanced rainfall on the African side (Hastenrath and Polzin, 2004). At 200 hPa, strong westerly wind anomalies are in the same direction as climatology implying strong upper level divergence. This is consistent with the initiating convective zone over coastal Tanzania, which suggests enhanced rainfall there. The

Fig. 4. El Niño composite OND anomaly fields OLR in (W/m^2), 850 hPa moisture flux in g/kg · m/s and 700 hPa and 200 hPa wind in m/s for **a**) pre-onset (P – 1), **b**) onset (P0), **c**) peak (P1) and **d**) withdrawal (P + 1) pentads. Scale vectors are shown and shading represents negative OLR anomalies

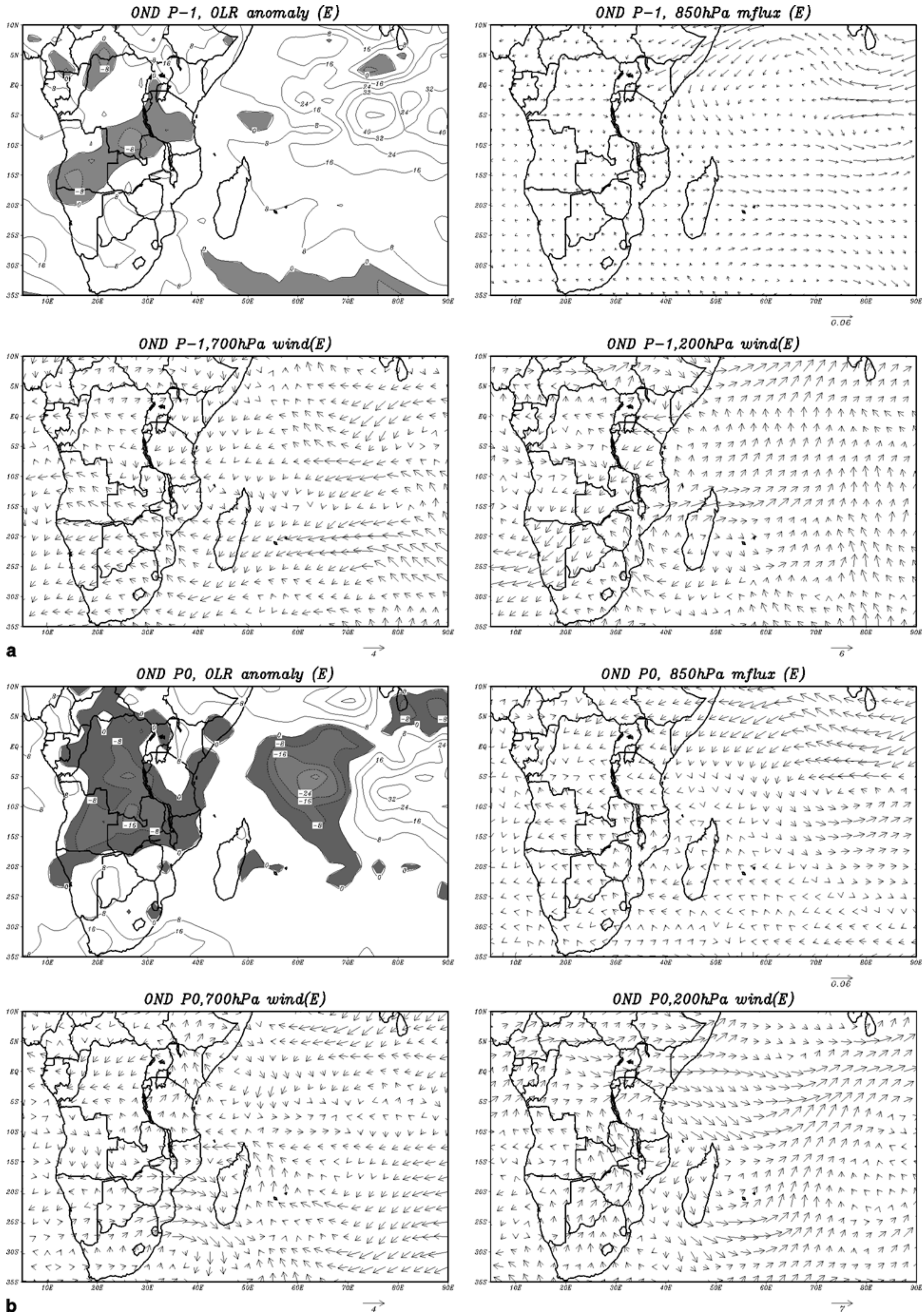
OND P-1, OLR anomaly (E)
OND P-1, 850hPa mflux (E)
OND P-1,700hPa wind(E)
OND P-1,200hPa wind(E)
a
OND P0, OLR anomaly (E)
OND P0, 850hPa mflux (E)
OND P0,700hPa wind(E)
OND P0,200hPa wind(E)
b

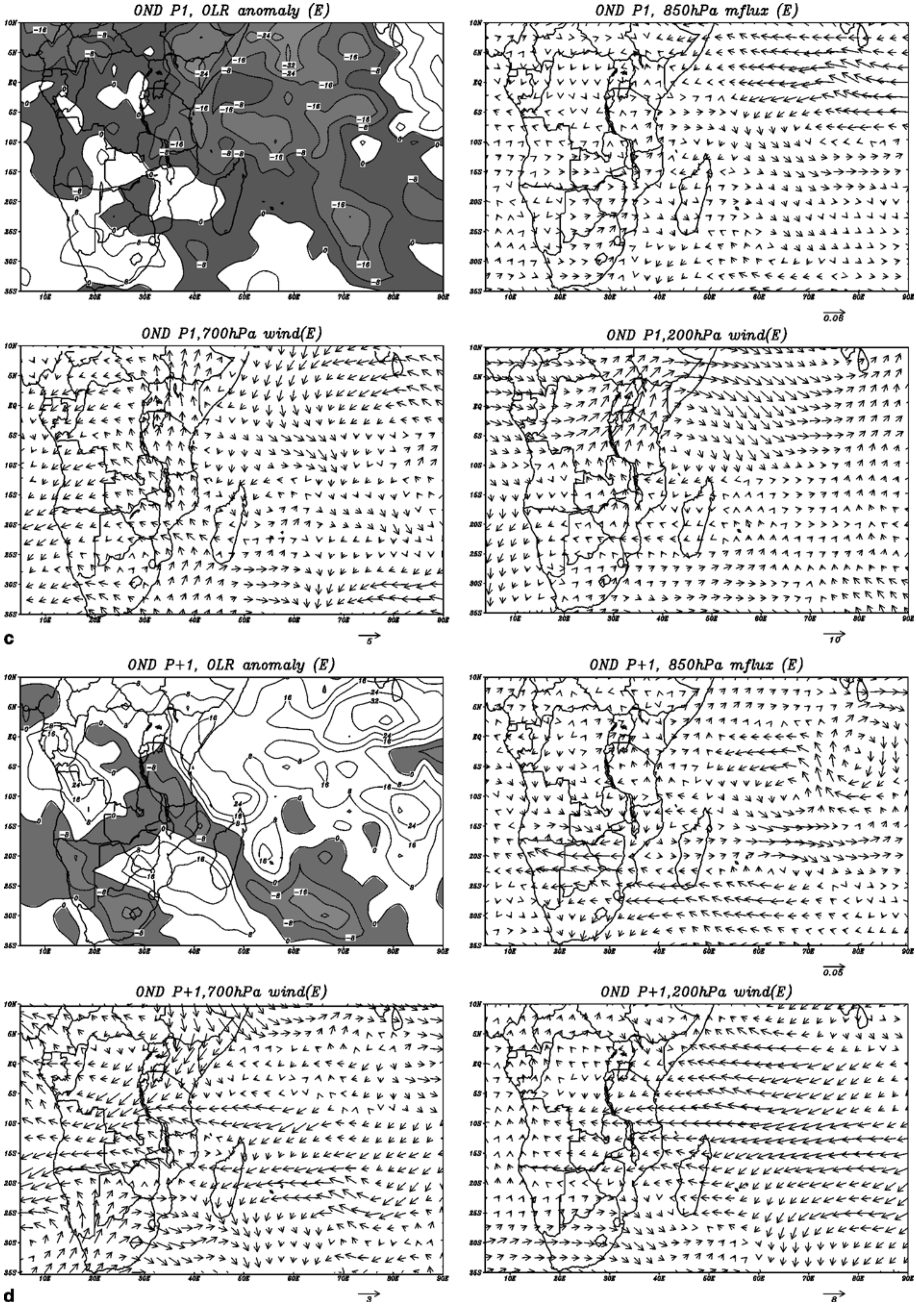

Fig. 4 (*continued*)

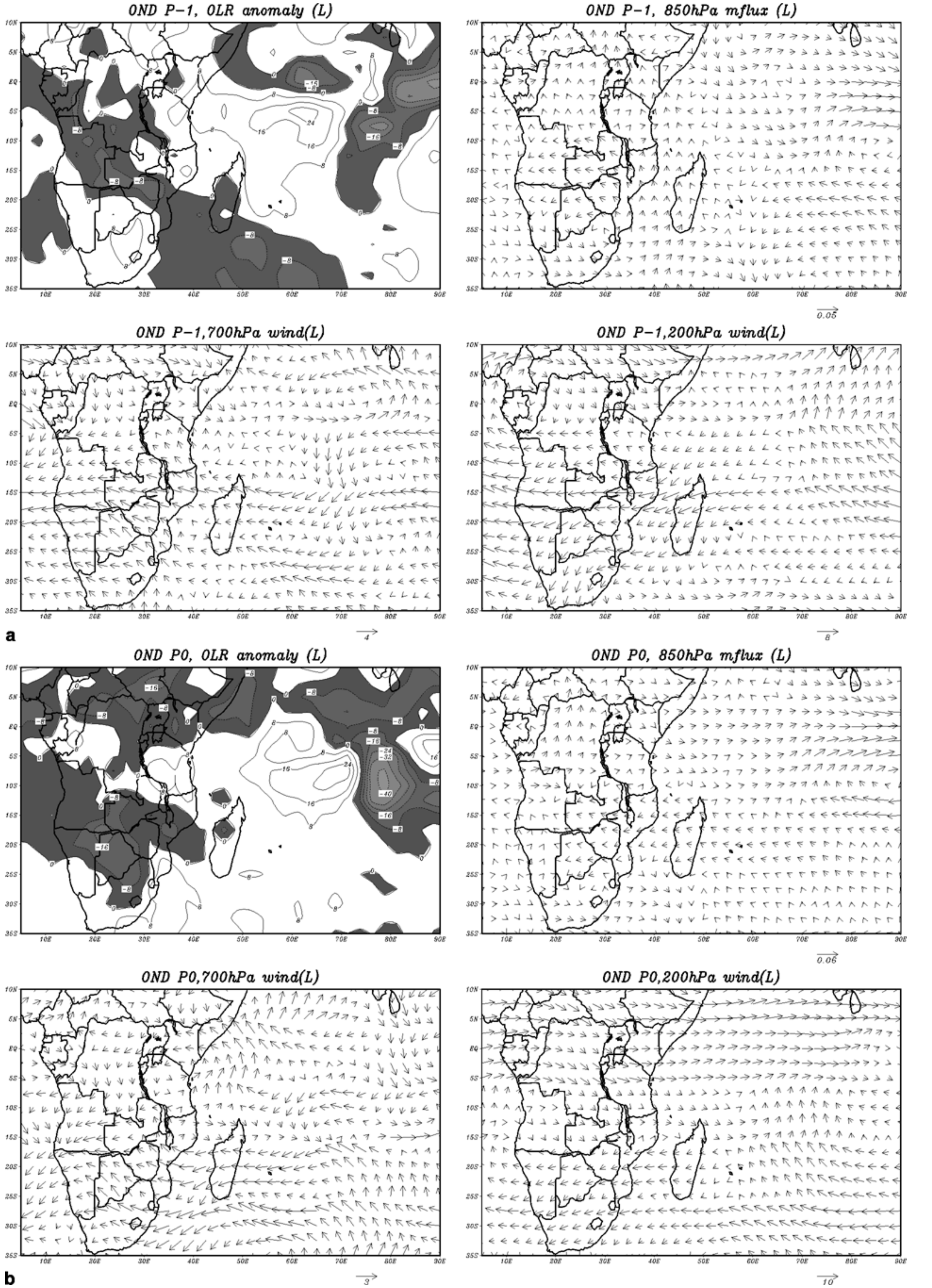

Fig. 5. La Niña composite OND anomaly fields OLR in $(\mathrm{W/m^2})$, 850 hPa moisture flux in $\mathrm{g/kg \cdot m/s}$ and 700 hPa and 200 hPa wind in m/s for **a**) pre-onset $(\mathrm{P}-1)$, **b**) onset (P0), **c**) peak (P1) and **d**) withdrawal $(\mathrm{P}+1)$ pentads. Scale vectors are shown and shading represents negative OLR anomalies

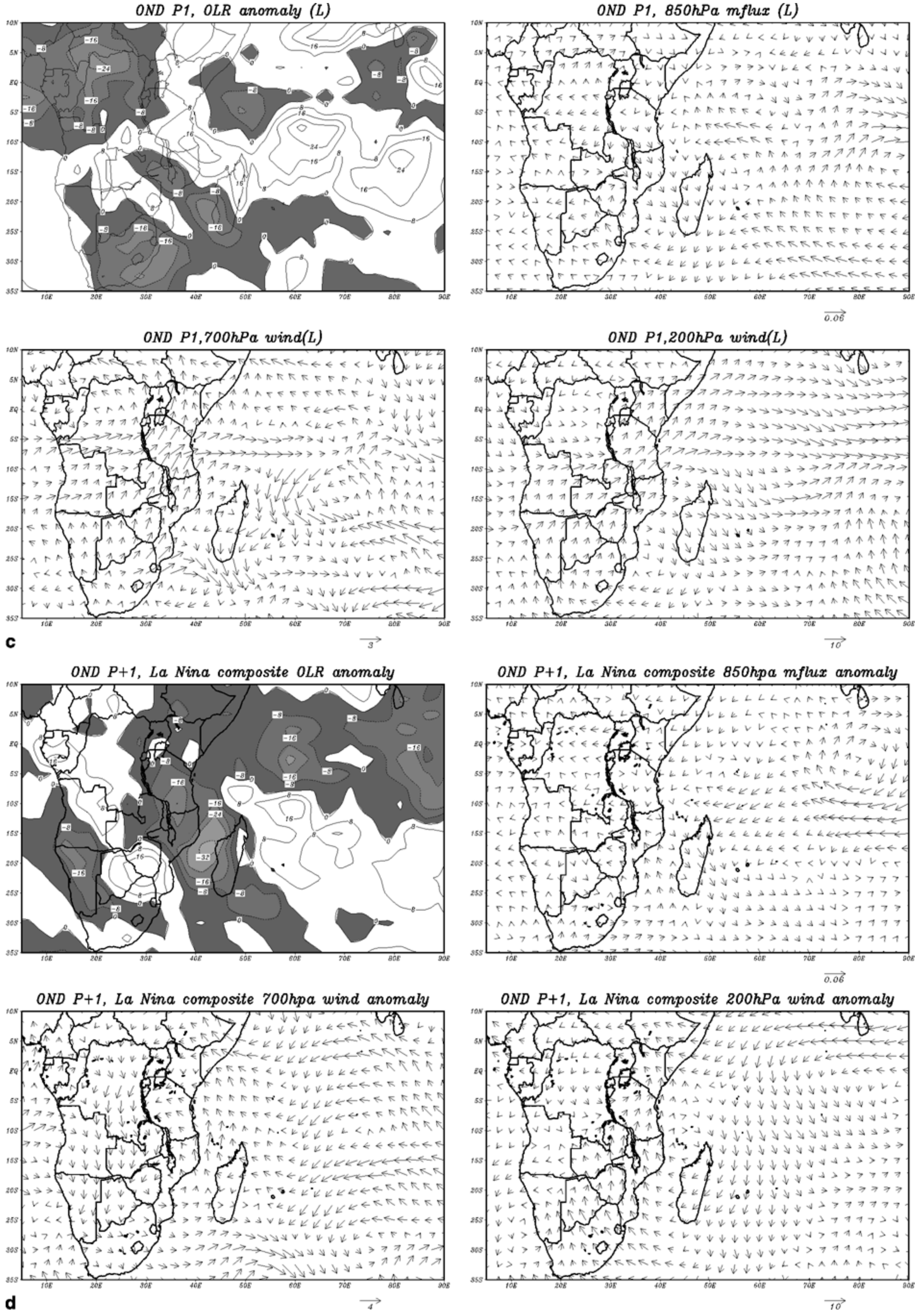

Fig. 5 (*continued*)

presence of an active convective zone over the equatorial western Indian Ocean with enhanced moisture convergence results in above average rainfall over the Tanzanian coast during El Niño years.

At the peak of OND rain season (P1) (Fig. 4c), the convective zone over the western Indian Ocean shows significant westward extent and has merged with that initiated over coastal East Africa during the onset (Fig. 4b). Over coastal Tanzania, negative OLR anomalies of about -15 to $-20\,\mathrm{W/m^2}$ are apparent. The area between 10° N and 5° S over the central Indian Ocean shows low-level easterly moisture flux anomalies and easterly anomalies at 700 hPa opposing the climatological export of moisture away from East Africa by the equatorial westerlies, consistent with negative OLR anomalies over the region and enhanced rainfall (Hastenrath and Polzin, 2004). Much of Tanzania and the nearby ocean indicates a westerly moisture flux anomaly, which converges with the easterly moisture flux anomaly at about 55° E. Since the mean moisture flux over Tanzania during this time is easterly, the westerly moisture flux anomaly tends to oppose the flow causing deceleration and enhanced moisture convergence over the coast. This convergence leads to the peak of rain during this pentad of above average rainfall. Moisture convergence over the Indian Ocean at about 55° E with stronger negative OLR anomalies over the region coupled with divergence at 200 hPa (not shown) indicates the position of the rising limb of Indian Ocean Walker cell, which shows a significant westward shift towards East Africa.

At the end of the OND rain season $(P+1)$ (Fig. 4d), the convective zone over the western Indian Ocean is replaced by periods of clear weather as is evident from the positive OLR anomalies covering the tropical western Indian Ocean, the Tanzanian north coast and Kenya. The moisture flux anomaly over much of the equatorial western Indian Ocean indicates a relative divergent pattern as it flows in the same sense as the climatological flow, leading to more moisture advected towards 50° E and increased export from this region back over the ocean north and east of Madagascar. Relative convergence occurs over Zambia, southern Tanzania and northern Mozambique as the flow anomalies are in the opposite direction to the mean flow. This period marks the shift towards the summer rainy season over southern Africa as indicated by negative OLR anomalies over this part of the landmass. Subsiding conditions and reduced clouds occur over the Tanzanian coast with divergence in the lower levels as suggested by the moisture flux anomalies and convergence in the upper levels. The latter is implied by the wind flow pattern at 200 hPa that opposes the mean flow. These circulation patterns mark the end of the rainy season over equatorial East Africa.

The corresponding anomalies for the various pentad stages of the OND La Niña composite are given in Fig. 5a–d. One pentad before the onset of OND season $(P-1)$ (Fig. 5a), the La Niña composite is more or less the reverse of the El Niño composite with negative OLR anomalies over the equatorial central Indian Ocean coupled with enhanced westerly moisture flux which feeds the convection there. The presence of offshore (westerly) moisture flux anomalies over the Tanzanian coast suggests suppressed moisture advection one pentad prior to the onset of rainfall season. At 200 hPa, the winds represent a strengthening of the mean, and hence divergence, near the negative OLR anomaly, promoting convection and suggesting that the position of the rising limb of Walker cell is located over the equatorial central/eastern Indian Ocean consistent with negative OLR anomalies apparent over this part of the ocean. As discussed in Hastenrath (2000), an enhanced Indian Ocean Walker cell in the OND season tends to occur during La Niña.

During the onset of the OND rain season (P0) (Fig. 5b), the negative OLR anomalies over the central Indian Ocean are strengthened, and shifted further east, reaching approximately $-40\,\mathrm{W/m^2}$ at 80° E. This location contrasts with the El Niño onset situation (Fig. 4b) where the developing convection shifts west towards Africa and is located near 55–65° E. Most of Tanzania shows positive OLR anomalies suggesting reduced cloud and convection compared to average. At 850 hPa, westerly moisture flux anomalies exist over much of the Indian Ocean, which feed the convective zone centered at about 80° E and increasing the climatological export of moisture away from East Africa. This offshore moisture flux results in reduction of rainfall over the Tanzanian coast during La Niña years. Strong westerly anomalies are particularly evident at 850 hPa in the equatorial Indian Ocean consistent with a strong zonal pressure gradient and reduced (enhanced) rains over East Africa (Indonesia) (Hastenrath and Polzin, 2004). The ascending limb of the Walker cell over the central Indian Ocean strengthens as indicated by enhanced westerly moisture flux at 850 hPa with enhanced westerly winds at 200 hPa and hence divergence (not shown).

At the peak of the OND rain season (P1) (Fig. 5c), positive OLR anomalies are observed over the Tanzanian coast with highest values of 15–20 W/m^2 indicating suppressed convection over the coast. Negative anomalies are evident over countries further south, consistent with the enhanced rainfall generally experienced over much of southern Africa during La Niña. The moisture flux anomaly plot is roughly the reverse of the El Niño composite with ongoing westerly moisture flux anomalies over the western equatorial Indian Ocean and easterly anomalies north of Madagascar and near the Tanzanian coast. The northeasterly moisture flux anomaly over the coast represents acceleration relative to climatology resulting in moisture flux divergence and reduction of rainfall, which is consistent with positive OLR anomalies over the region. At 700 hPa, there are strong westerly anomalies over the Tanzanian coast enhancing the mean flow, implying divergence. Divergence at these middle levels (not shown) weakens the vertical extent of the convection and results in reduced rainfall.

At the end of the OND rain season (P + 1) (Fig. 5d), negative OLR anomalies are apparent over most of the tropical Indian Ocean and southeastern Africa indicating a strengthened Walker cell over the Indian Ocean and reduced uplift over Kenya and northern Tanzania. In addition, strong negative OLR anomalies are evident over the Mozambique region consistent with the developing wet conditions over southeastern Africa associated with La Niña. Weak northeasterly to northerly moisture flux anomalies exist near the Tanzanian coast with relative divergence, marking the end of the rainfall season here.

5.2 ENSO influence on the long rains (MAM)

One pentad before the onset of the MAM rainy season, (P – 1) (Fig. 6a), a convective zone is apparent over the equatorial western Indian Ocean (negative OLR anomalies). The other area of significant negative OLR anomaly east of Madagascar is too far south to be associated with the ITCZ. Westerly moisture flux anomalies over the equatorial North Indian Ocean feed the equatorial convective zone. The enhanced equatorial westerlies at 700 hPa relative to climatology suggest that the mid-level moisture flux also contributes to this developing convection. The upper level wind patterns show convergence (not shown) over much of the Tanzanian coast suggesting subsidence, and hence reduced cloud one pentad before the onset of the rain season.

During onset (P0) (Fig. 6b), the negative OLR anomalies over the equatorial Indian Ocean extend westwards towards the Tanzanian coast consistent with the southeasterly moisture flux anomaly just off the coast that opposes the mean flow. The ascending convective limb is over the equatorial western Indian Ocean as indicated by negative OLR anomalies and moisture convergence over the region coupled with upper level wind divergence (not shown). The enhanced moisture convergence over the equatorial western Indian Ocean results in increased rainfall over the coast during MAM season of the mature phase El Niño years.

At the peak of the season (P1) (Fig. 6c), negative OLR anomalies over the western Indian Ocean deepen reaching a minimum anomaly value of $-25\,W/m^2$ centered at 50–55° E and show the westward extent of convection, which covers the entire north coast of Tanzania. A cyclonic moisture flux anomaly exists over the equatorial western Indian Ocean with westerly moisture flux anomaly across southern Tanzania. This leads to enhanced moisture convergence

Fig. 6. El Niño + 1 composite MAM anomaly fields OLR in (W/m^2), 850 hPa moisture flux in $g/kg \cdot m/s$ and 700 hPa and 200 hPa wind in m/s for **a**) pre-onset (P – 1), **b**) onset (P0), **c**) peak (P1) and **d**) withdrawal (P + 1) pentads. Scale vectors are shown and shading represents negative anomalies

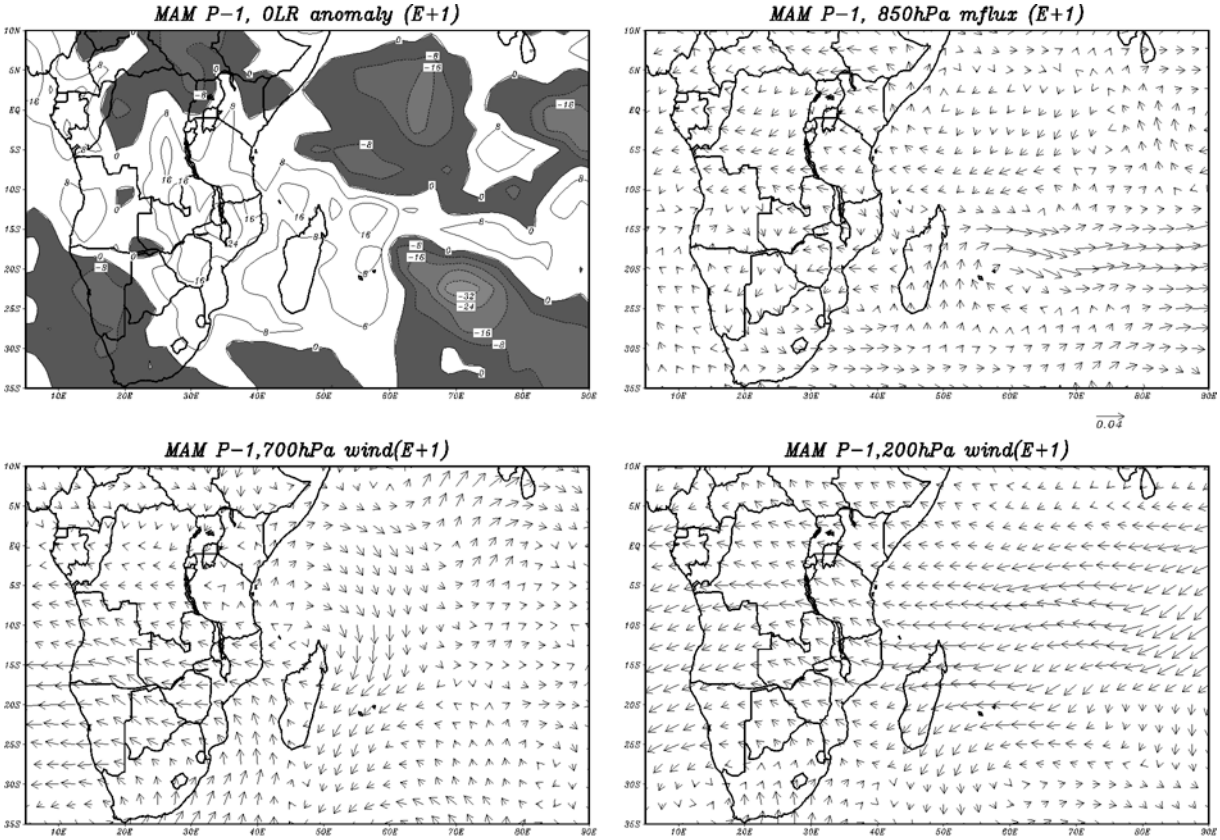
MAM P-1, OLR anomaly (E+1)
MAM P-1, 850hPa mflux (E+1)
0.04
MAM P-1,700hPa wind(E+1)
5
MAM P-1,200hPa wind(E+1)
10

a

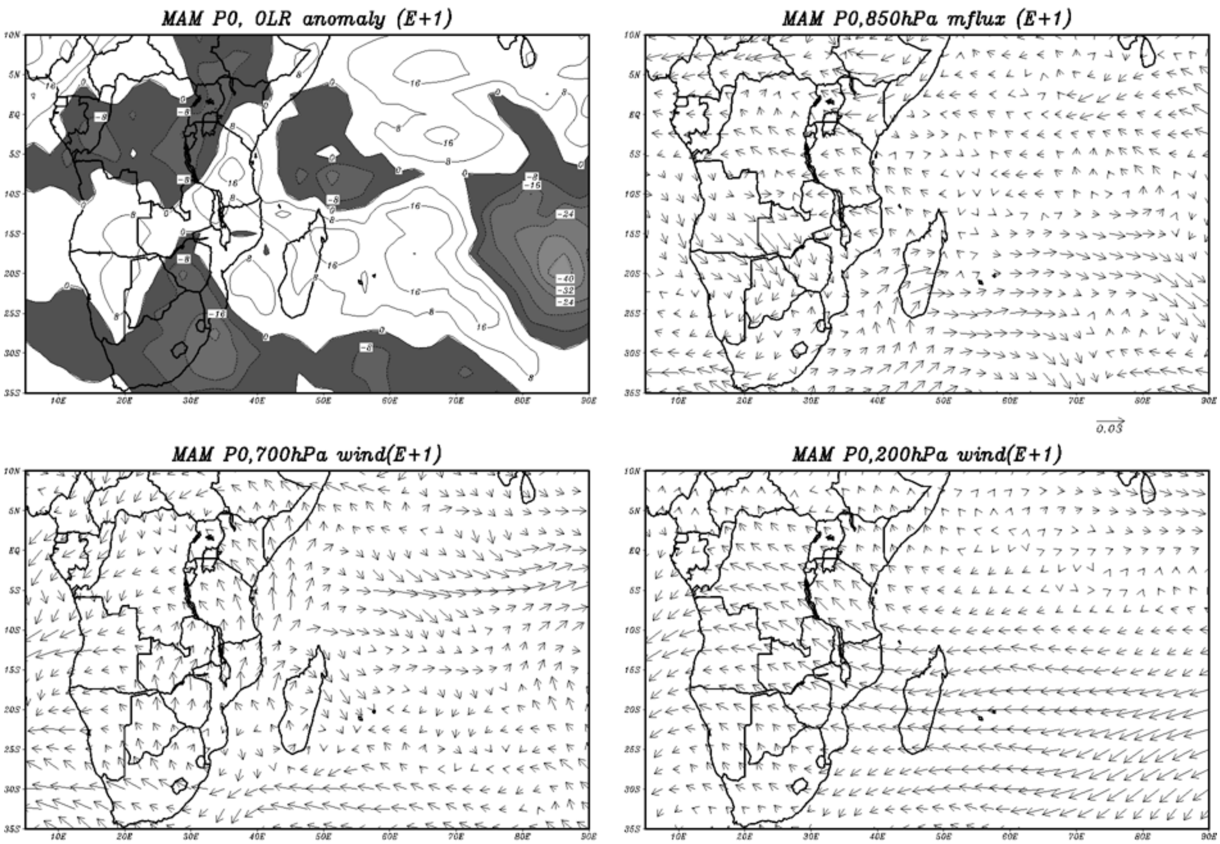
MAM P0, OLR anomaly (E+1)
MAM P0,850hPa mflux (E+1)
0.03
MAM P0,700hPa wind(E+1)
3
MAM P0,200hPa wind(E+1)
10

b

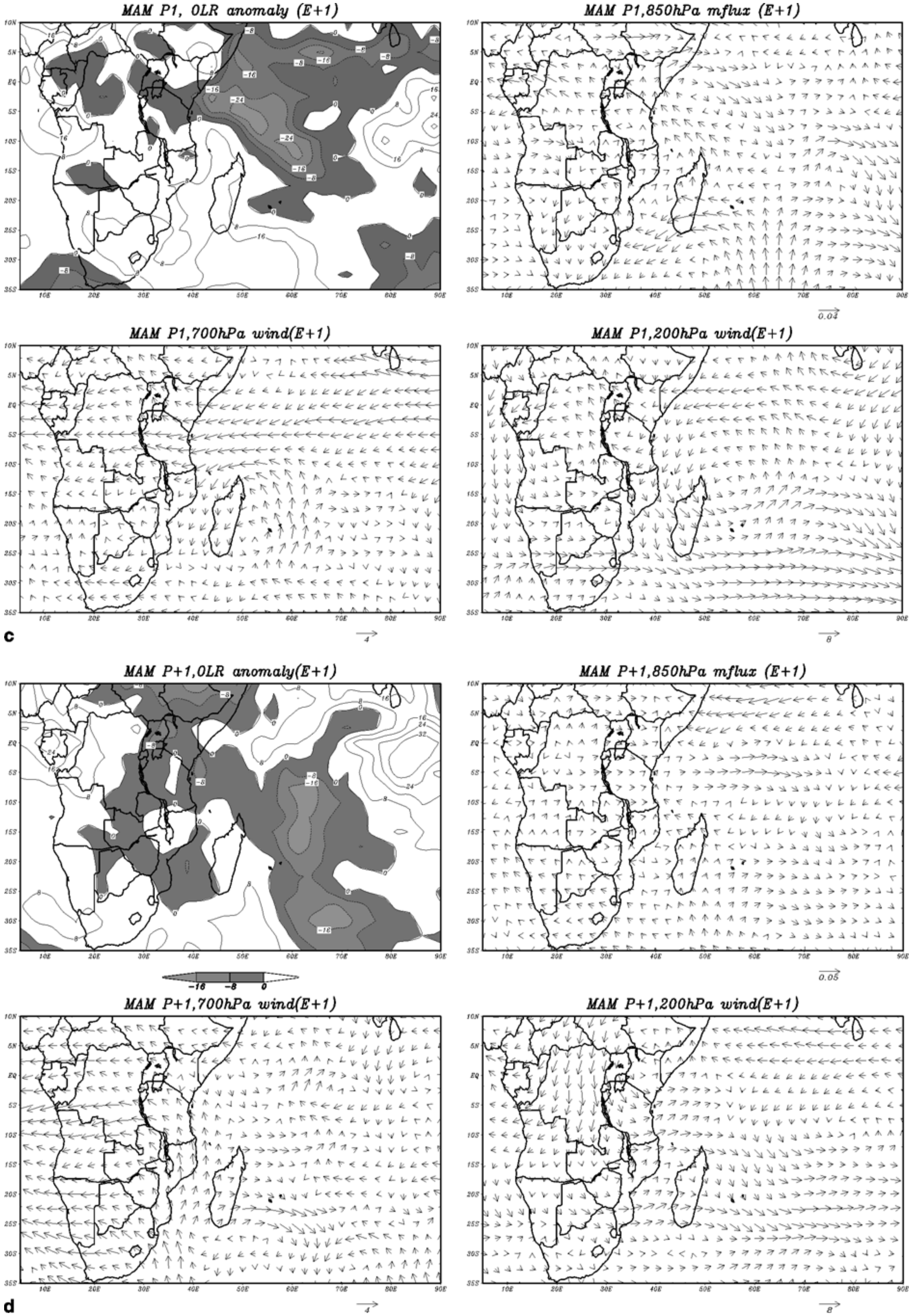

Fig. 6 (*continued*)

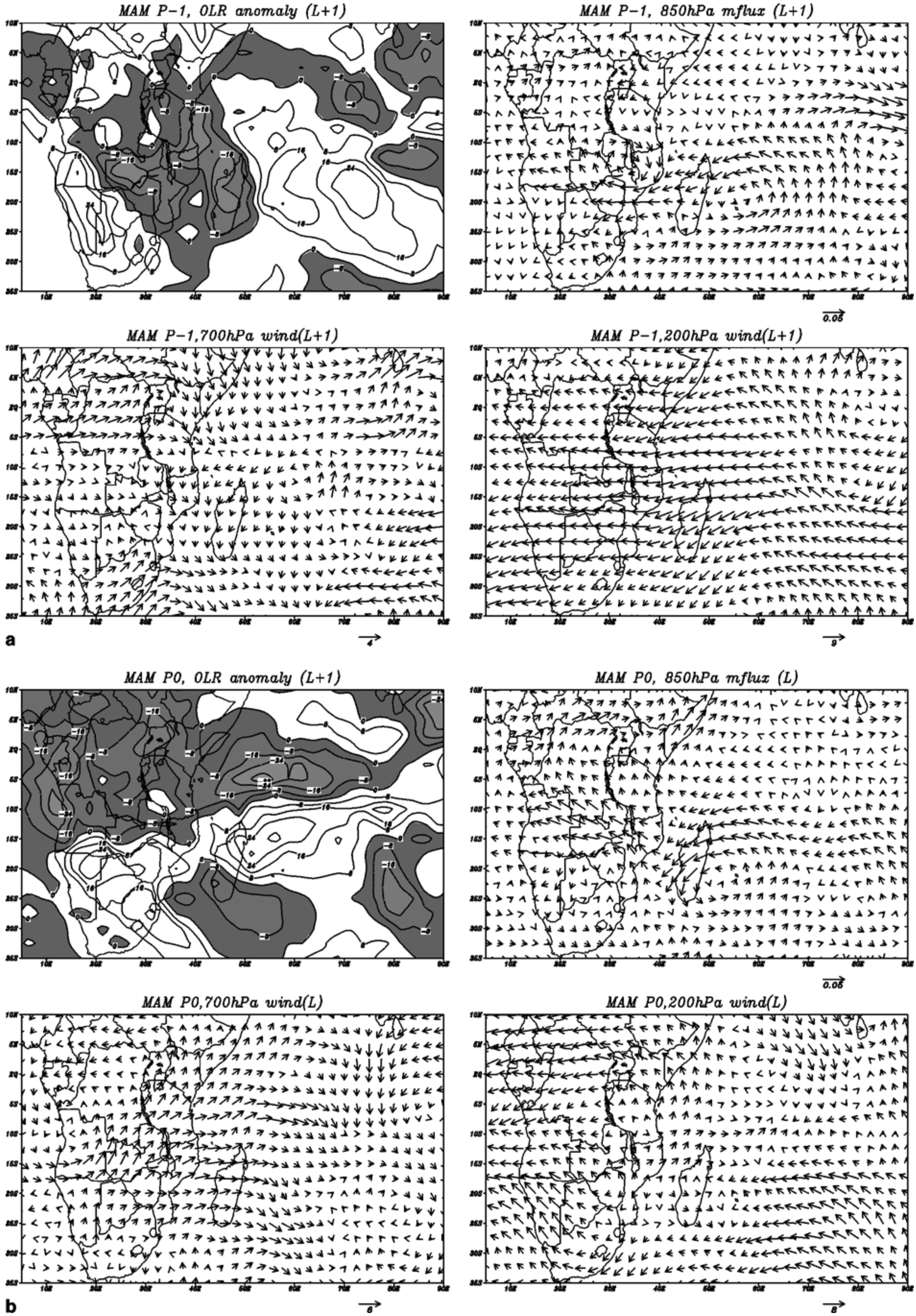

Fig. 7. La Niña + 1 composite OND anomaly fields OLR in $(\mathrm{W/m^2})$, 850 hPa moisture flux in $\mathrm{g/kg \cdot m/s}$ and 700 hPa and 200 hPa wind in m/s for **a**) pre-onset (P − 1), **b**) onset (P0), **c**) peak (P1) and **d**) withdrawal (P + 1) pentads. Scale vectors are shown and shading represents negative anomalies

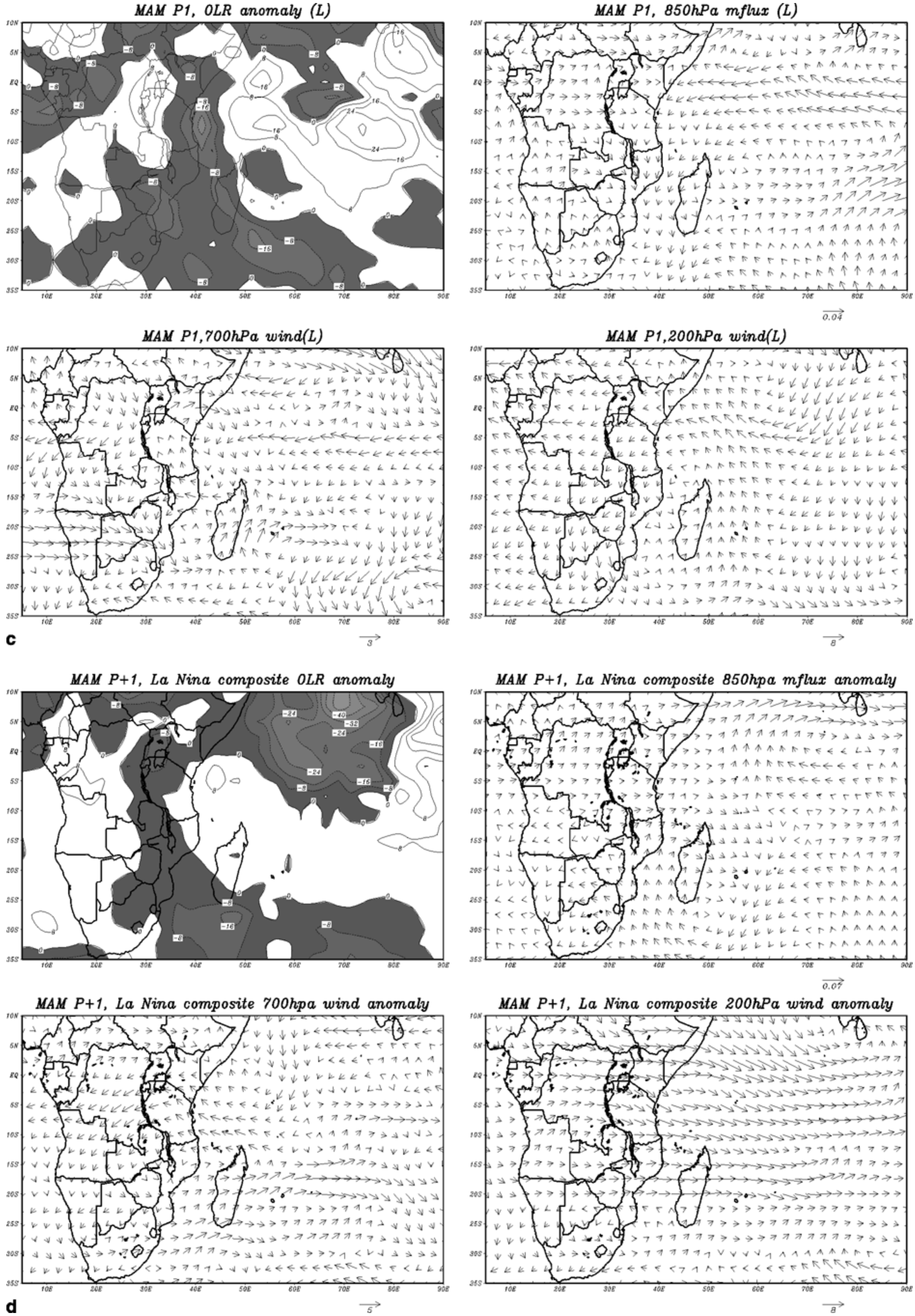

Fig. 7 (*continued*)

over much of Tanzania (not shown) and increased rainfall marking the peak of rainfall season over the Tanzanian coast. The 700 hPa wind shows an anticyclonic anomaly centered over Madagascar with strong easterly anomalies over the tropical western Indian Ocean and Tanzania opposing the background flow, hence reducing the climatological export of moisture away from East Africa. This anticyclonic anomaly shows an equatorward shift with height and, at 200 hPa, it is located over the tropical western Indian Ocean thereby indicating the position of the ascending convective limb.

During withdrawal (P + 1) (Fig. 6d), the convective zone over the equatorial western Indian Ocean shows an eastward shift leaving weak negative anomalies over the Tanzanian north coast. The cyclonic moisture flux anomaly over the equatorial western Indian Ocean is less apparent and a south equatorial westerly moisture flux anomaly, which feeds the maritime convective zone, is evident. The descending limb of the convective cell is located over the equatorial western Indian Ocean as indicated by positive OLR anomalies over this region with wind convergence at 200 hPa (not shown) implying reduced cloud cover. This marks the end of the rainfall season over the Tanzanian coast.

The corresponding anomalies for the MAM La Niña + 1 composite are now discussed. One pentad before the onset of MAM rain season (P − 1) (Fig. 7a), negative OLR anomalies cover eastern Tanzania and southeastern Africa and positive OLR anomalies are located east and north of Madagascar. An anticyclonic moisture flux anomaly is evident over the Indian Ocean east of Madagascar. The northerly to northwesterly moisture flux anomalies over the Tanzanian coast are in the same direction as the mean flow implying moisture flux divergence. The convective zone over the Tanzanian coast is short-lived since there is upper level wind convergence (not shown), which implies descending motion over the region.

At onset (P0) (Fig. 7b), a dipole pattern in OLR anomalies exists over the Indian Ocean with positive anomalies south of 10° S and negative anomalies to the north. Most of Tanzania shows weak negative OLR anomalies. The anticyclonic moisture flux anomaly east of Madagascar shows a slight westward shift, which allows easterly moisture flux anomalies to dominate much of the western Indian Ocean between the equator and about 25° S. As a result, the moisture flux anomaly over the Tanzanian coast is the same sense as the mean flow and therefore divergent, leading to reduction of rainfall. At 700 hPa, there are strong southwesterly anomalies over tropical Africa and the western Indian Ocean that feed into the equatorial convective zone offshore, but lead to mid-level convergence (not shown) over Tanzania, subsidence, and less rain.

During the peak of the season (P1) (Fig. 7c), negative OLR anomalies are observed over the Tanzanian coast consistent with low level moisture flux convergence over the region (not shown). However, the development of deep convective clouds is unlikely since the upper level wind anomalies are relatively strong easterlies, opposing the mean flow, and leading to convergence at 200 hPa (not shown) and hence subsidence. Below average rainfall over the Tanzanian coast is evident during this period.

Towards the withdrawal of the season (P + 1) (Fig. 7d), a convective zone develops over the northwest Indian Ocean with relatively strong westerly moisture flux anomalies at 850 hPa feeding the convection. These suggest that the developing monsoon over the northwest Indian Ocean may be initially stronger than average and the ITCZ has moved northwards more quickly than typical. The descending limb of the convective cell is located over East Africa, with reduced cloud there as indicated by positive OLR anomalies near the coast. This marks the end of rainfall season over the northern coast of Tanzania.

6. Summary and conclusion

This study has outlined some of the important dynamical patterns underlying the intraseasonal variability of rainfall over the Tanzanian coast. Focus has been placed on the north part (4–8° S) of the coast which shows a coherent ENSO impact; the signals over the south coast are less clear and appear to be a transition between the opposite responses over East and southern Africa. The climatological onset, peak and rainfall withdrawal plots confirm the association of Tanzanian coast rainfall with the migration of the ITCZ. The peak of the rainfall season is found to occur while the ITCZ is over the region.

Hovmöller and pentad analyses revealed a coherent temporal and spatial relationship between the enhanced and suppressed convection associated with intraseasonal oscillations during ENSO years. The rainfall time series for the north coast revealed that increased rainfall during El Niño OND seasons was associated with an early onset, less dry spells and more intense rainfall whereas reduced rainfall during La Niña years was associated with a late start of the season, more dry spells and less intense rains. For MAM, the El Niño seasons tended to start late as did most of the La Niña seasons. Rainfall impacts were less clear in MAM than for OND. A possible explanation for this may be because the ENSO-induced oceanic Rossby wave that propagates the signal across the Indian Ocean leads to a negative feedback between this wave, the overlying winds and SST in the post-mature phase MAM season whereas for the preceding OND season, the feedback with the atmosphere is positive and the SST signal is more robust (Xie et al., 2002). Thus, Fig. 6c, which corresponds to the peak pentad of the MAM rainy season shows a low level cyclonic anomaly north of Madagascar implying a damping of the El Niño-induced SST warming via Ekman divergence and upwelling. Conversely, the low level anticyclonic anomaly south of India during the peak phase of the OND rainy season (Fig. 4c) implies Ekman convergence and hence amplification of the developing warm SST anomaly during this phase of ENSO. This anticyclonic anomaly extends towards East Africa and is co-located with increased rainfall over the western Indian Ocean. As a result, ENSO impacts over Tanzania are more likely to die out quickly in MAM, or not be coherent if the timing of the event is shifted relative to the annual cycle, leading to a less obvious relationship between north coast rainfall and ENSO during this season.

Increased rainfall over the north coast during El Niño years was observed to be associated with enhanced convection and moisture flux convergence over the Tanzanian coast and reduced export of moisture away from East Africa over the equatorial western Indian Ocean. La Niña years tend to show the reverse. Consistent with Hastenrath and Polzin (2004), there are weakened (strengthened) equatorial westerlies over the central Indian Ocean during El Niño (La Niña) with signs of weaker (stronger) south-easterly trades. The wet conditions of the OND season of the El Niño onset years are extended to the usually dry months of January and February of the mature phase El Niño year.

The OLR and zonal wind Hovmöller plots revealed eastward and westward propagating as well as stationary features over the Indian Ocean. It was observed that the propagating features tended to be absent during strong El Niño years whereas for strong La Niña years, they are often present. It is also found that the areas of large negative OLR anomalies (strong convection) tend to couple well with areas of strong westerly anomalies in lower levels with strong easterly anomalies in the upper levels. Westward propagating negative OLR anomalies are found over the far western Indian Ocean during El Niño OND seasons and are associated with strong convection over the Tanzanian coast and increased rain while the reverse is observed during La Niña. Further east over the Indian Ocean, eastward propagating features are evident during El Niño whereas the signals are less clear for La Niña. For the MAM season, some years show westward propagating features over the central and western Indian Ocean (e.g. 1983, 1987) whereas others show eastward propagation (e.g. 1995, 1998).

The onset and peak of rainfall during El Niño years are found to be associated with an active convective zone over the equatorial western Indian Ocean with enhanced moisture convergence, which results in above average rainfall while the reverse is true for La Niña years. In conclusion, ENSO has a significant influence on intraseasonal rainfall over the north Tanzanian coast, particularly for OND. For the south coast, the signals are similar to the north coast and the rest of East Africa for OND, but for the other half of the rainy season (JFM), mixed ENSO signals are evident.

Acknowledgements

This study was done when the first author was at the University of Cape Town on a Third World Organization for Women in Science (TWOWS) fellowship. Dr. D. Jagadheesha offered useful support on computing and plotting during the preparation of a MSc thesis by the first author, from which this paper derives. The NCEP/NCAR data obtained from their website http://www.cdc.noaa.gov are gratefully acknowledged. Rainfall data were kindly supplied by the Tanzania Meteorological Agency. We thank the reviewers for helpful comments which improved the paper.

References

Alusa AL, Gwange PM (1978) The occurrence of dry spells during the East African long rains. Research report No. 5/78, E.A Institute for Meteorology, pp 1–18

Amissah-Arthur A, Jagtap S, Rosenzweig C (2002) Spatio-temporal effects of El Niño events on rainfall and maize yield in Kenya. Int J Climatol 22: 1849–1860

Anyamba EK (1992) Some properties of a 20–30 day oscillation in tropical convection. J Afr Met Soc 1: 1–19

Cadet DL (1985) The Southern Oscillation over the Indian Ocean. J Climatol 5: 189–212

Camberlin P (1995) June–September rainfall in north-eastern Africa and atmospheric signals over the tropics: a zonal perspective. Int J Climatol 15: 773–783

Doblas-Reyes FJ, Déqué M (1998) A flexible bandpass filter design procedure applied to midlatitude intraseasonal variability. Mon Wea Rev 126: 3326–3335

Hastenrath S, Nicklis A, Greischar L (1993) Atmospheric hydrospheric mechanisms of climate anomalies in the western equatorial Indian Ocean. J Geophys Res 98(C 11): 20219–20235

Hastenrath S (2000) Zonal circulations over the equatorial Indian Ocean. J Climate 13: 2746–2756

Hastenrath S, Polzin D (2004) Dynamics of the surface wind field over the equatorial Indian Ocean. Quart J Roy Meteor Soc 130: 503–517

Hayashi Y, Golder DG (1993) Tropical 40–50 and 25–30 day oscillations appearing in realistic and idealized GFDL climate models and the ECMWF dataset. J Atmos Sci 50: 464–494

Hutchinson P (1992) The Southern Oscillation and prediction of "Der" season rainfall in Somalia. J Climate 5: 525–531

Indeje M, Semazzi FHM, Ogallo LJ (2000) ENSO signals in East African rainfall seasons. Int J Climatol 20: 19–46

Janowiak (1988) An investigation of Inter annual rainfall. J Climate 1: 240–255

Kabanda TA, Jury MR (2000) Synoptic evolution of composite wet spells over northern Tanzania. Climate Res 15: 239–248

Kalnay E, and Co-authors (1996) The NCEP/NCAR 40-year Reanalysis Project. Bull Amer Meteor Soc 77: 437–471

Knutson TR, Weickmann KM (1987) 30–60 day atmospheric circulations: Composite life circles of convection and circulation anomalies. Mon Wea Rev 115: 1407–1436

Levey KM, Jury M (1996) Composite intra-seasonal oscillations of convection over southern Africa. J Climate 9: 1910–1920

Madden RA, Julian PR (1971) Detection of a 40–50 day oscillation in the zonal wind in the tropical Pacific. J Atmos Sci 28: 702–708

Madden RA, Julian PR (1994) Observations of the 40–50 day tropical oscillation: a review. Mon Wea Rev 122: 814–837

Matarira CH, Jury MR (1992) Contrasting Meteorological structure of Intra seasonal wet and dry spells in Zimbabwe. Int J Climatol 12: 165–176

Mhita MS (1984) The use of water balance models in the optimation of cereal yields in seasonally-arid tropical regions. PhD Thesis. University of Reading, p 211

Mhita MS, Nassib IR (1987) The onset and end of rain in Tanzania. Proc. 1st Tech. Conference. Meteor Res Eastern and Southern Africa, Nairobi, pp 101–115

Mpeta EJ, Jury MR (2001) Intra-seasonal convective structure and evolution over tropical East Africa. Climate Res 17: 83–92

Mutai CC, Ward MN (2000) East African rainfall and the tropical circulation/convection on intraseasonal to interannual timescales. J Climate 13: 3915–3939

Nicholson SE (1996) A review of climate dynamics and climate variability in Eastern Africa. In: Johnson TC, Odata E (eds) Limnology, climatology and paleoclimatology of the East African lakes. The Netherlands: Gordon and Breach Publishers

Nicholson SE, Kim J (1997) The relationship of the El Niño-Southern Oscillation to African Rainfall. Int J Climatol 17: 117–135

Nyenzi BS (1988) Mechanisms of East African Rainfall variability. PhD. Thesis Florida State University, 184 pp

Ogallo LJ (1988) Relationship between seasonal rainfall in East Africa and Southern Oscillation. J Climatol 8: 34–43

Ogallo LJ (1989) The spatial and temporal patterns of the East African seasonal rainfall derived from principal component analysis. Int J Climatol 9: 145–167

Reason CJC, Allan RJ, Lindesay JA, Ansell TA (2000) ENSO and climatic signals across the Indian Ocean basin in the global context. Int J Climatol 20: 1285–1327

Ropelewski CF, Halpert MS (1987) Global and regional scale precipitation patterns associated with the El Niño-Southern Oscillation. Mon Wea Rev 115: 1606–1626

Rui H, Wang B (1990) Development characteristics and dynamic structure of tropical intraseasonal convection anomalies. J Atmos Sci 47: 357–379

Saji NH, Goswami BN, Vinayachandran PN, Yamagata T (1999) A dipole mode in the tropical Indian Ocean. Nature 401: 360–363

Tourre YM, White WB (1997) Evolution of ENSO signal over the Indo-Pacific domain. J Phys Oceanogr 27: 683–696

Vincent DG, Sperling T, Fink A, Zube S, Speth P (1991) Intraseasonal oscillation of convective activity in the tropical Southern Hemisphere: May, 1984-April, 1986. J Climatol 4: 40–53

Webster PJ, Moore AM, Loschnigg JP, Lebden RR (1999) Coupled ocean–atmosphere dynamics in the Indian Ocean during 1997–98. Nature 401: 356–360

Wheeler MA, Kiladis GN (1999) Convectively coupled equatorial waves: analysis of clouds and temperature in the wavenumber-frequency domain. J Atmos Sci 56: 374–399

Wheeler MA, Weickmann KM (2001) Real-time monitoring and prediction of modes of coherent synoptic to intraseasonal tropical variability. Mon Wea Rev 129: 2677–2694

Xie P, Arkin PA (1997) Global precipitation: A 17-year monthly analysis based on gauge observations, satellite estimates and numerical model outputs. Bull Amer Meteor Soc 78: 2539–2558

Xie S-P, Annamalai H, Schott FA, McCreary JP (2002) Structure and mechanism of South Indian Ocean climate variability. J Climate 15: 864–878

Zhu B, Wang B (1993) The 30–60 day convective seesaw between the tropical Indian and western Pacific Oceans. J Atmos Sci 50: 184–199

Authors' addresses: Agnes L. Kijazi*, C. J. C. Reason (e-mail: cjr@egs.uct.ac.za), Department of Oceanography, University of Cape Town, Rondebosch 7701, South Africa. *Also at: Tanzania Meteorological Agency, P.O. Box 3056 Dar es Salaam, Tanzania.